CLRC

Technical Report
RAL-TR-97-010

Crystalline Si diodes as Neutron Detectors: Test Measurements at the ISIS Pulsed Neutron Source

C Petrillo F Sacchetti N J Rhodes and M W Johnson

February 1997

COUNCIL FOR THE CENTRAL LABORATORY OF THE RESEARCH COUNCILS

Enquiries about copyright, reproduction and requests for additional copies of this report should be addressed to:

The Central Laboratory of the Research Councils
Library and Information Services
Rutherford Appleton Laboratory
Chilton
Didcot
Oxfordshire
OX11 0QX
Tel: 01235 445384 Fax: 01235 446403
E-mail library@rl.ac.uk

ISSN 1358-6254

Technical Report
RAL-TR-97-010

CLRC

Crystalline Si diodes as Neutron Detectors: Test measurements at the ISIS Pulsed Neutron Source

C. Petrillo, F. Sacchetti, N.J. Rhodes and M.W. Johnson.

January 1997

COUNCIL FOR THE CENTRAL LABORATORIES OF THE RESEARCH COUNCIL

Crystalline Si diodes as Neutron Detectors: Test measurements at the ISIS Pulsed Neutron Source.

C. Petrillo,[*] F. Sacchetti,[*] N.J. Rhodes [+] and M.W. Johnson.[+]

[*]Istituto Nazionale per la Fisica della Materia, Unita' di Perugia, Perugia, Italy and Dipartimento di Fisica, Universita' di Perugia, Via A. Pascoli, 06100 Perugia, Italy.

[+]Rutherford Appleton Laboratory, Chilton, Didcot, Oxon. OX11 0QX U.K.

Abstract

Test measurements have been carried out on a prototype solid state neutron detector; a crystalline Si diode coupled to a Gd converter. The experiment was performed on the PEARL beam line at ISIS to investigate the performance of the device when operated on a pulsed neutron source. A measurement of the γ-sensitivity was made by exposing the detector to a standard ^{60}Co source. The neutron detection efficiency was measured at several neutron wavelengths and found to be in very good agreement with the results of a previous Monte Carlo simulation.

1. Introduction

Within the framework of **ENNI** (European Network for Neutron Instrumentation), the use of semiconductor devices as neutron detectors has been investigated. At present, the best candidate is a crystalline Si diode sensor coupled to a Gd converter. Exploiting the current developments in both Si diode fabrication technology and VLSI readout electronics [1,2], two prototype neutron detectors have been assembled and tested (Fig. 1). The performance of these two detectors was measured at the Trigger reactor in Rome using a clean double-monochromatic thermal neutron beam (λ = 1.2 Å). These results have been extensively discussed [3, 4] and are summarised in Table 1. Neutron detection efficiency as a function of neutron wavelength and converter thickness for different converter-diode configurations, was simulated by means of a Monte Carlo algorithm. Neutron detection efficiency of a 10 μm thick Gd converter measured at λ = 1.2 Å was well reproduced by a Monte Carlo calculation when the experimental arrangement of the sensor was taken into account. To confirm the Monte Carlo conclusions additional measurements of the response of the device to neutrons of different wavelengths was sought, together with an experimental test of the γ-sensitivity.

Neutron test measurements were carried out on the PEARL beam line at ISIS. The Si detector and a standard ZnS scintillator reference detector [5] were used to measure the diffraction patterns of some standard samples simultaneously. Neutron detection efficiencies at various neutron wavelengths were calculated from a comparative analysis of the data collected by both the diode and the scintillator. Finally, a measurement of the γ-sensitivity was carried out by exposing the detector to a 600 kBq ^{60}Co source situated 2.5 cm from the detector. The present experimental results add more information to the previous measured data and confirm the validity of the Monte Carlo simulation.

2. Neutron measurements

The Si detector prototype and the readout electronics have been described previously [3, 4]. For the present measurements a 5 mm x 4 mm diode, 300 μm thick was used as shown in Fig. 1b. An 18 mm x 18 mm Gd foil, 10 μm thick was mounted on an aluminium frame. The distance between the converter foil and the Si sensor was adjustable to enable this distance to be minimised. A fixed distance of 1 mm was maintained, compatible with the microbonds on the diode surface. The converter, diode and front-end monolithic amplifier were contained in an aluminium alloy box with a 2 mm wall thickness.

The output from the diode was connected to a standard ORTEC amplifier and a single channel analyser (SCA). The amplifier output was sent to a pulse height analyser (PHA) card (SILENA SpA, Milan) installed on an IBM-PC while the SCA output was sent to the standard ISIS DAE through a TTL/NIM converter. The energy spectra of conversion electrons were collected by the PHA simultaneously with the time of flight (ToF) data acquisition. The DAE was sent signals within the electron energy range 35-240 keV by appropriate setting of the SCA low level and window discriminators. Fig. 2 shows a typical conversion electron spectrum collected at the PHA during ToF data acquisition.

In Fig. 3 a schematic drawing of the experimental setup on PEARL is shown. The ZnS scintillator detector, with a 20 mm x 20 mm active area, was mounted behind the diode box and slightly off center. Common shielding of both detectors was arranged using B_4C plates and wax blocks. A B_4C mask with a 30 mm x 60 mm hole was placed on the face of the diode box to act as a collimator. All the samples were mounted at sample position 1 on the PEARL line corresponding to moderator to sample distance of 12.6 m. The scattering angle was fixed at 90° for all the measurements, but one, with a sample to detector distance of ~0.4 m. Diffraction patterns of some reference samples were measured, namely an incoherent scatterer, a single crystal, a powder and an amorphous sample. Background measurements were

performed using either B_4C or ^6Li glass as neutron absorbers placed in front of the B_4C collimator.

2.1 Incoherent scatterer

The wavelength spectrum of a perspex rod (5 cm in diameter and 10 cm high) as recorded by both the diode and the scintillator detectors is shown in Fig. 4. From a qualitative inspection of Fig. 4, an estimate of the intensity ratio between the two detectors can be obtained. In the thermal region this ratio is ~20. Thus the intensity is roughly proportional to the detector area (20 mm x 20 mm ZnS and 5 mm x 4 mm Si). Obtaining a more accurate value for the expected detector ratio requires attenuation effects due to the aluminium box, the readout card and the Gd foil to be taken into account. Neutrons impinging on the scintillator are mainly attenuated by the Gd foil although this only covers a portion of the scintillator area.

Background measurements were obtained by leaving the perspex sample in place and covering the detector collimator hole by a B_4C plate 1 cm thick. In this case an intensity ratio close to 1 was found from the ZnS and Si ToF spectra. Such a result suggests that boron compounds may present problems when used as shielding materials since the Si diode seems to be sensitive to the cascade of γ-rays produced by neutron absorption in boron. The previously obtained intensity ratio of ~20 was recovered in the background measurements when ^6Li glass (~1 cm thick) was used in place of the B_4C plate.

2.2 Single crystal

The diffraction pattern of a cylindrical lead single crystal 2.5 cm diameter and 5 cm high with the vertical axis parallel to the (0 0 1) direction was measured. The ToF data are shown in Fig. 5. The diffraction pattern of (h 0 0) Bragg reflections extending from (2 0 0) to (10 0 0) was obtained with the ZnS scintillator detector. The highest order observed using the Si detector was (8 0 0). This corresponds to an incoming neutron wavelength λ = 0.87 Å. Such a wavelength represents the lower operational limit of the diode, below which the neutron detection efficiency of the Gd converter sharply decreases. Because of the high counting rate, dead-time corrections must be applied to the intensity collected by the scintillator. A dead-time of ~2 μs was assumed. Such a correction is important when evaluating the neutron detection efficiency of the diode by reference to that of the scintillator.

2.3 Powder samples

A sample of Fe powder, contained in a cylindrical thin walled (0.1 mm) vanadium can (5 mm diameter, 80 mm in length), was measured and the ToF spectra are compared in Fig. 6a. The diffraction pattern of the Si detector shows the (3 2 1) Bragg reflection as the highest order reflection. This corresponds to $\lambda = 1.08$ Å.

In Fig. 6b the ToF spectra of a barium fluoride polycrystal (5 mm diameter, 20 mm in length) also contained in a thin walled vanadium can are presented. The BaF_2 measurements were carried out while trying to reduce the effects of possible background sources. In particular, the sample area was evacuated and the B_4C collimator in front of the detector box helped in reducing the background by ~20%.

2.4 Amorphous sample

A ribbon of amorphous $Fe_{81}B_{13.5}Si_{3.5}C_2$ was chosen as an example of a disordered and low intensity sample. The ribbon, 0.025 mm thick and 50 mm wide, was rolled to produce a hollow cylinder with a wall thickness of 0.6 mm. The measurement was performed at a scattering angle of 46° instead of 90°. The Fe powder sample was used to calibrate the new scattering angle. A reduction of the scattering angle was necessary to cover the region of wavevectors lower than ~2 $Å^{-1}$ where the important features of the amorphous static structure factor are expected. The raw data were normalized to the monitor and corrected by the monitor efficiency. In the case of ZnS, the data were also corrected by the scintillator efficiency (~20 % at 1 Å) and an additional correction for neutron attenuation by the Gd foil was applied. The attenuation was evaluated with reference to the geometric configuration and relative size of the Gd foil and ZnS scintillator. An effective attenuation of ~40 % over the thermal region was obtained. The data collected by the diode were corrected by the diode efficiency as deduced by the experimental spectra on Pb single crystal and Fe powder (see next section). The background was not measured at the 46° scattering angle and hence no background subtraction was applied to the data. The resulting intensities are shown in Fig. 7 as a function of the wavevector. The curves of Fig. 7 are intended for a qualitative inspection only. The point is that the main features of the spectrum as measured by ZnS are reproduced by the diode. The intensity, after scaling for the ZnS and Si surface areas, is roughly the same for both detectors.

3. Detection efficiency

The whole of the Bragg peak data collected on the Fe, BaF_2 polycrystal and Pb single crystal samples was used to deduce the neutron detection efficiency of the Si detector using the known ZnS efficiency as a reference. The Bragg peaks of the ToF spectra were fitted using Gaussian functions. The background was subtracted by a linear fit to the data on both sides of the Bragg peak. The centre of the Gaussian curves was used to deduce the neutron wavelength. The integrated intensity for each Bragg peak was calculated using the Gaussian curve corrected by background subtraction. The integrated intensity data obtained for the ZnS detector were additionally corrected for the Gd attenuation. A neutron detection efficiency for the ZnS detector of ~20 % at $\lambda \geq 1$ Å and a 1/v scaling law for its absorption cross section was assumed. The neutron detection efficiency of the Si detector was then deduced from the ratio of the integrated intensities per unit area for each Bragg peak simultaneously measured by the diode and the scintillator. In Fig. 8a the measured efficiency values of the Si detector are given as a function of neutron wavelength. The data deduced by the BaF_2 diffraction pattern exhibit large error bars mainly because of the low intensity of the Bragg peaks. On the other hand, the error on the efficiency values deduced by the Pb data is very small (of the same order of the dots in Fig. 8a). The very high intensity of the Bragg peaks from the Pb single crystal required the additional correction for the dead-time to be applied to the data collected by the ZnS detector. As mentioned, a dead-time of 2 μs was assumed and the corresponding integrated intensities were corrected for such an effect. An inspection of Fig. 8a shows that an efficiency of ~4 % is still found at $\lambda = 0.87$ Å and saturation values of ~20 % are observed for $\lambda \leq 2$ Å. The experimental data are shown in comparison with the efficiency curve calculated by the Monte Carlo algorithm described previously [3, 4]. The simulation program was run by setting the available input options to reproduce the experimental configuration. These were a 10 μm Gd converter thickness, a 1 mm converter to sensor distance, a 35-240 keV energy window and a Gd-Si transmission configuration. The agreement between the calculated curve and the experimental data is quite satisfactory thus confirming the reliability of the Monte Carlo simulation. A prediction of the best performance achievable by the Si sensor equipped with the Gd converter was obtained by an extensive Monte Carlo simulation [3, 4]. The results are shown in Fig. 8b for the optimum Gd thickness of 7 μm, the converter in close contact with the diode and an energy window from 40 keV to 150 keV. Efficiencies of the order of 40 % at $\lambda =$ 2 Å could be obtained with the optimized Gd-Si-Gd configuration. Finally, a test of the γ-sensitivity was carried out by exposing the detector box to a ^{60}Co source operated at 2.5 cm distance. The activity of the source in such a configuration was 32 mRem/hr, i.e. $\sim 2 \times 10^4$ photons s^{-1} cm^{-2}. From this measurements an efficiency of $\sim 10^{-5}$ was calculated.

Acknowledgments

This work was supported by the EC HCM programme through the European Network for Neutron Instrumentation (Contract No. CHRX-CT92-0006), by the ISIS facility, CCLRC (UK) and the University of Perugia (Italy).

References

[1] Proceedings of the Third London Conference on Position Sensitive Detectors}, (London, U. K., September 6-10, 1993) in Nuclear Instrum. and Methods A 348, 207-746 (1994).

[2] O. Toker, Proceedings 2nd International Meeting on Front-end Electronics for Tracking Detectors at Future High Luminosity Colliders (1994).

[3] C. Petrillo, F. Sacchetti, O. Toker and N. J. Rhodes, Nuclear Instrum. and Methods A. 378, 541-551 (1996)

[4] C. Petrillo, F. Sacchetti, O. Toker and N. J. Rhodes, J. Neut. Res., Proceedings of New Tools for Neutron Instrumentation, Les Houches (1995).

[5] N. J. Rhodes et al., Proceedings ICANS XII, RAL Report, RAL-94-025 1, 185 (1993).

Characteristic	Si diode	Si microstrip
Dead-time	1–5 μs	0.1 μs
Peaking time	1 μs	50 ns
Signal/noise	40	10
Position resolution	$\sim$ 40μm achievable	1 mm measured
Neutron detection efficiency	$\leq$ 20% at 1.2 Å with 10 μm Gd on one side	

Table I

Basic characteristics of the two prototype crystalline Si detectors from monochromatic neutron (λ = 1.2 Å) experiments [3, 4].

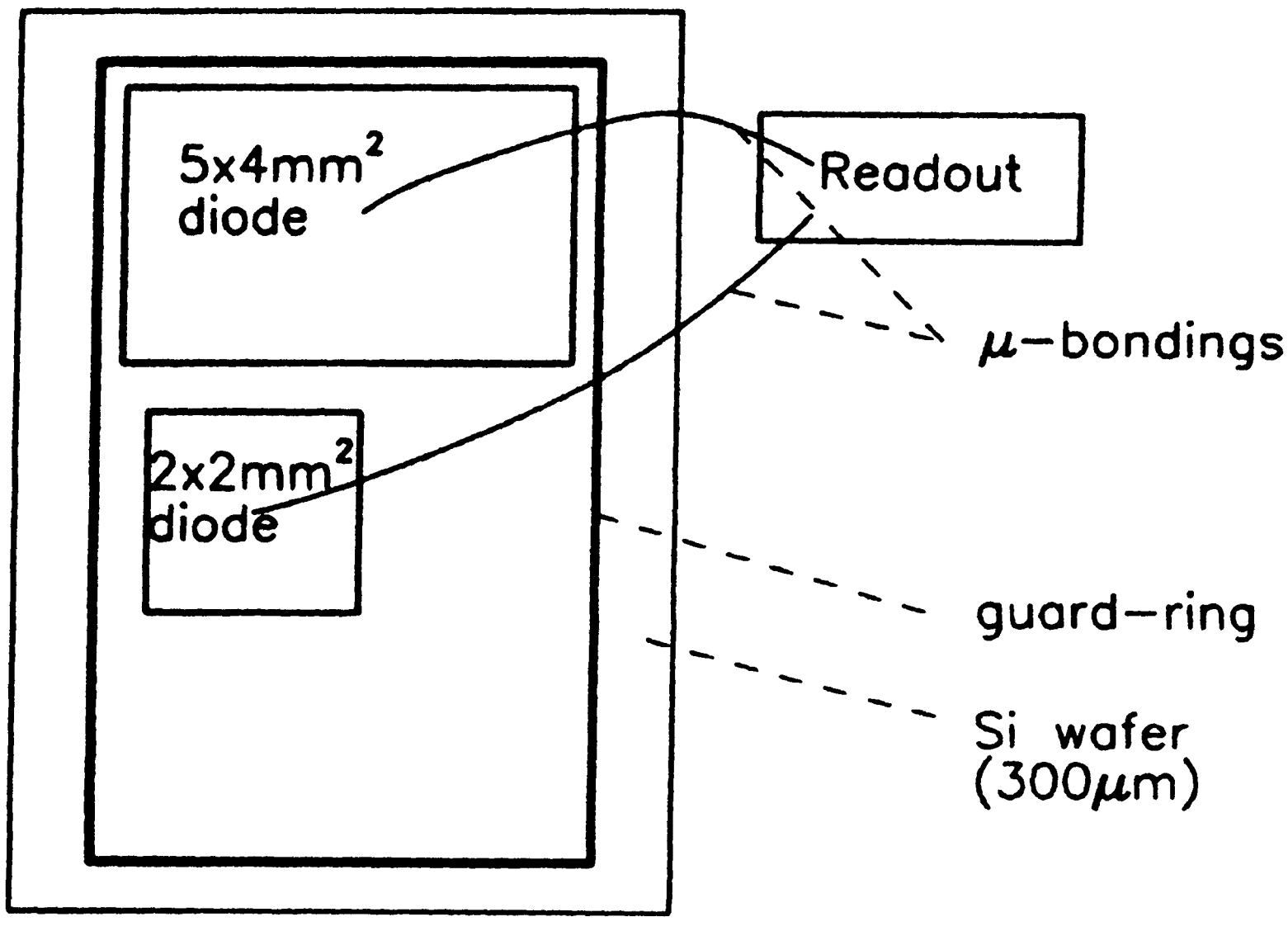

Figure 1. Diode sensor pattern of the Si detector.

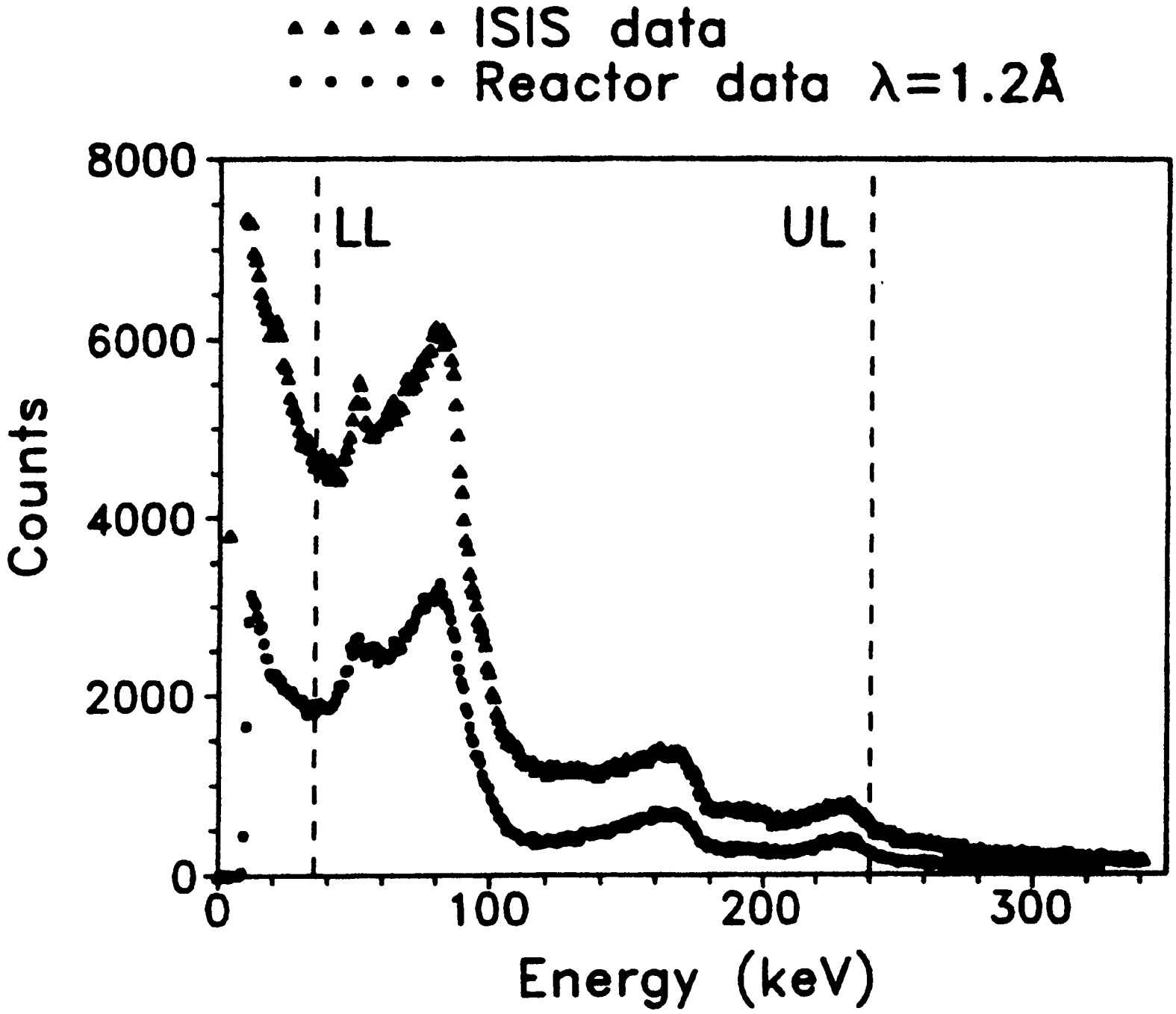

Figure 2. Typical pulse height spectrum of conversion electrons in Gd. Data collected at ISIS (triangles) are shown in comparison with the spectrum measured with monochromatic neutrons (λ = 1.2 Å) at the Trigger reactor in Rome (dots). Signals within the energy window defined by the dashed lines were sent to the DAE.

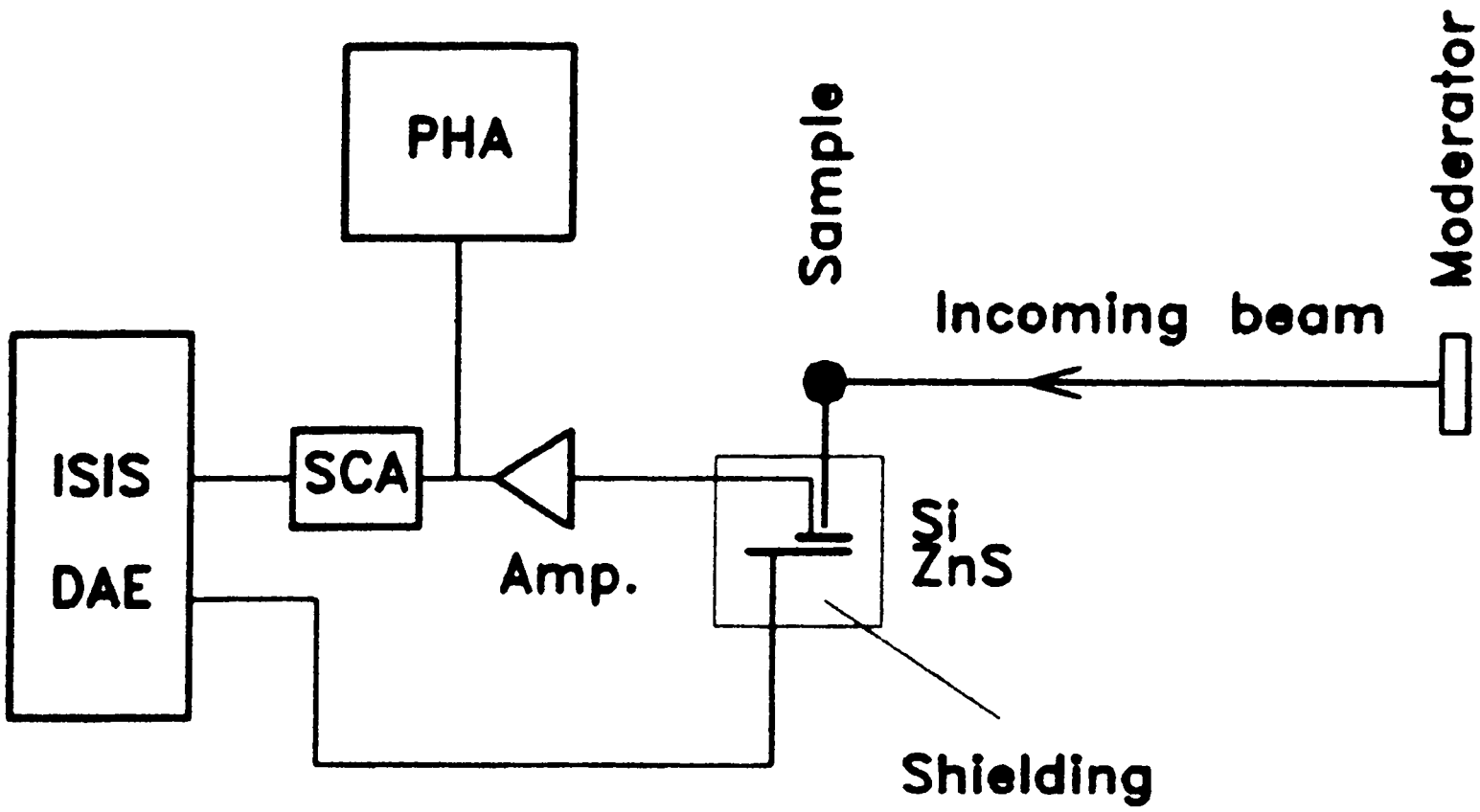

Figure 3. Schematic drawing of the experimental setup at the PEARL beam line

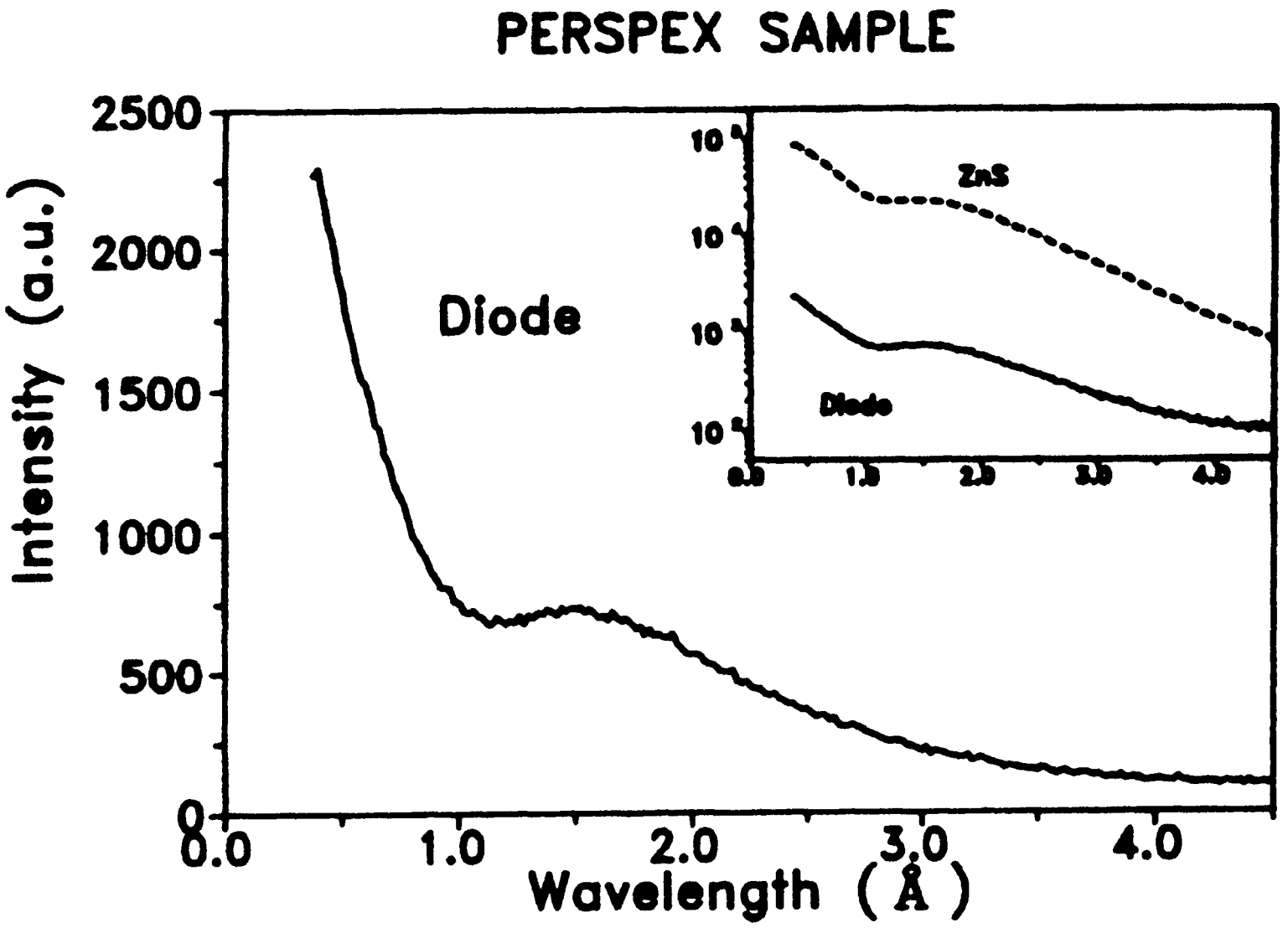

Figure 4. Wavelength spectrum from a perspex sample measured using the Si detector. ZnS scintillator and Si detector data are compared in the inset.

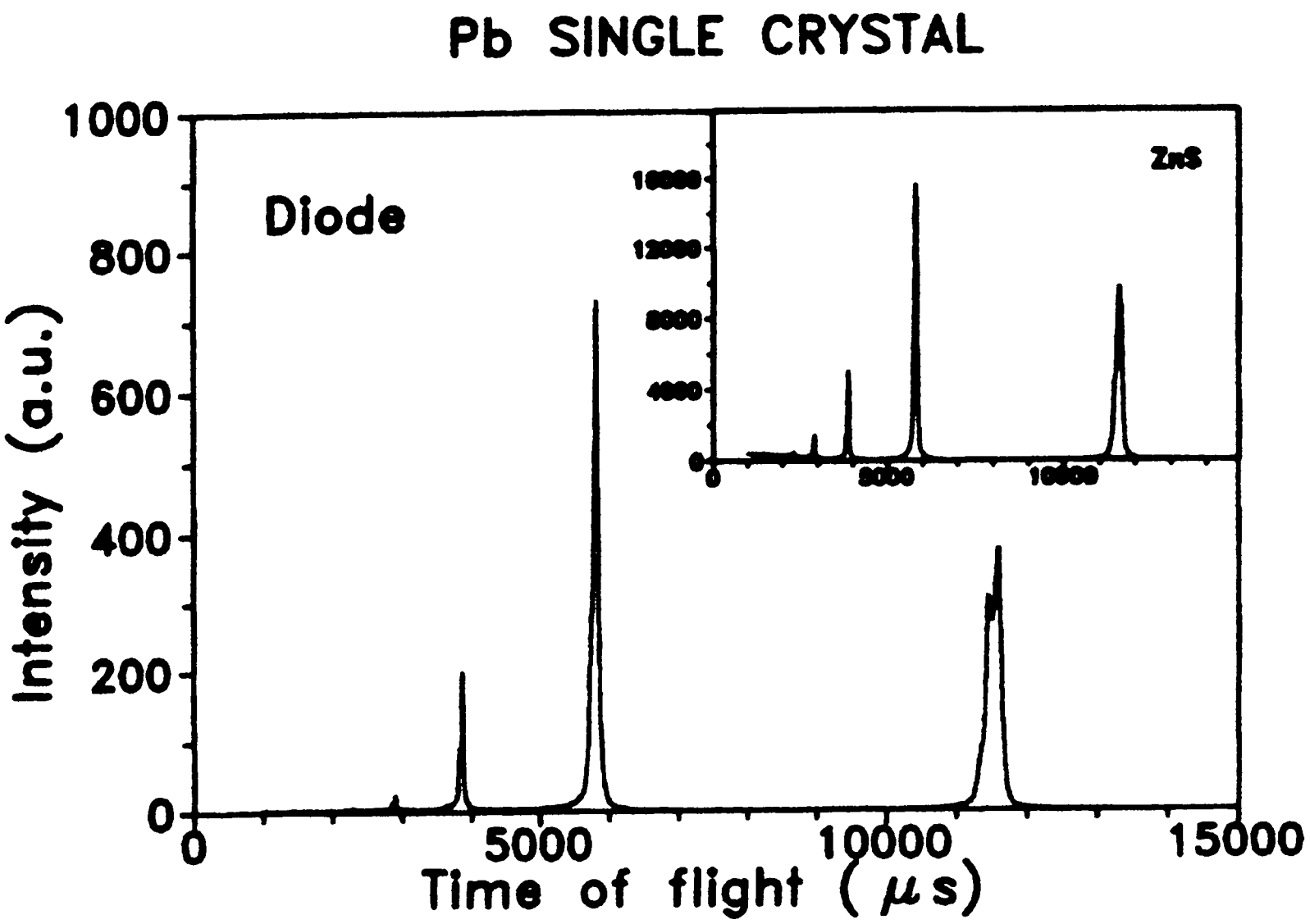

Figure 5. ToF spectrum from a Pb single crystal measured using the Si detector. Data collected using the ZnS scintillator are shown in the inset.

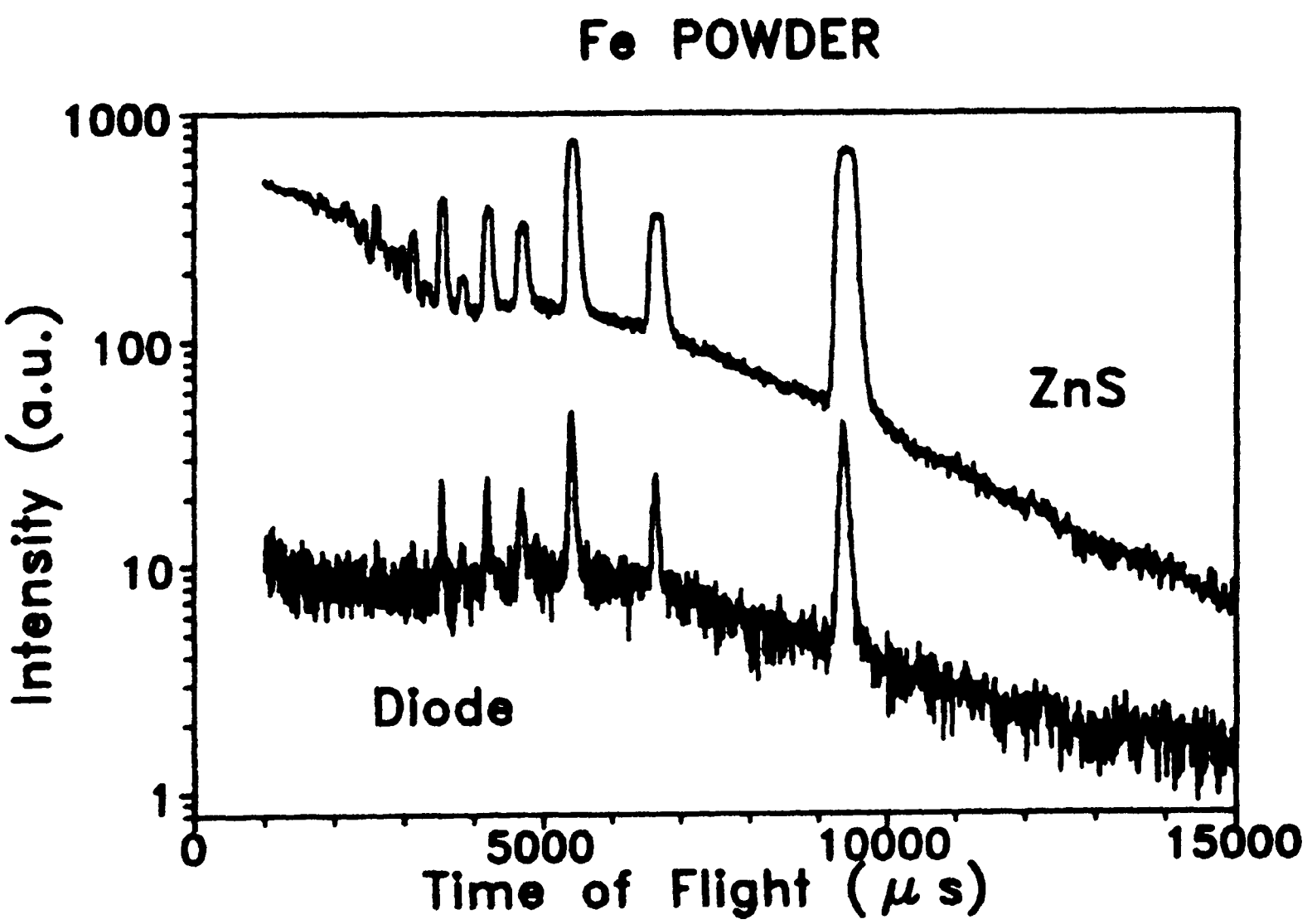

Figure 6a. ToF spectra from the Fe powder.

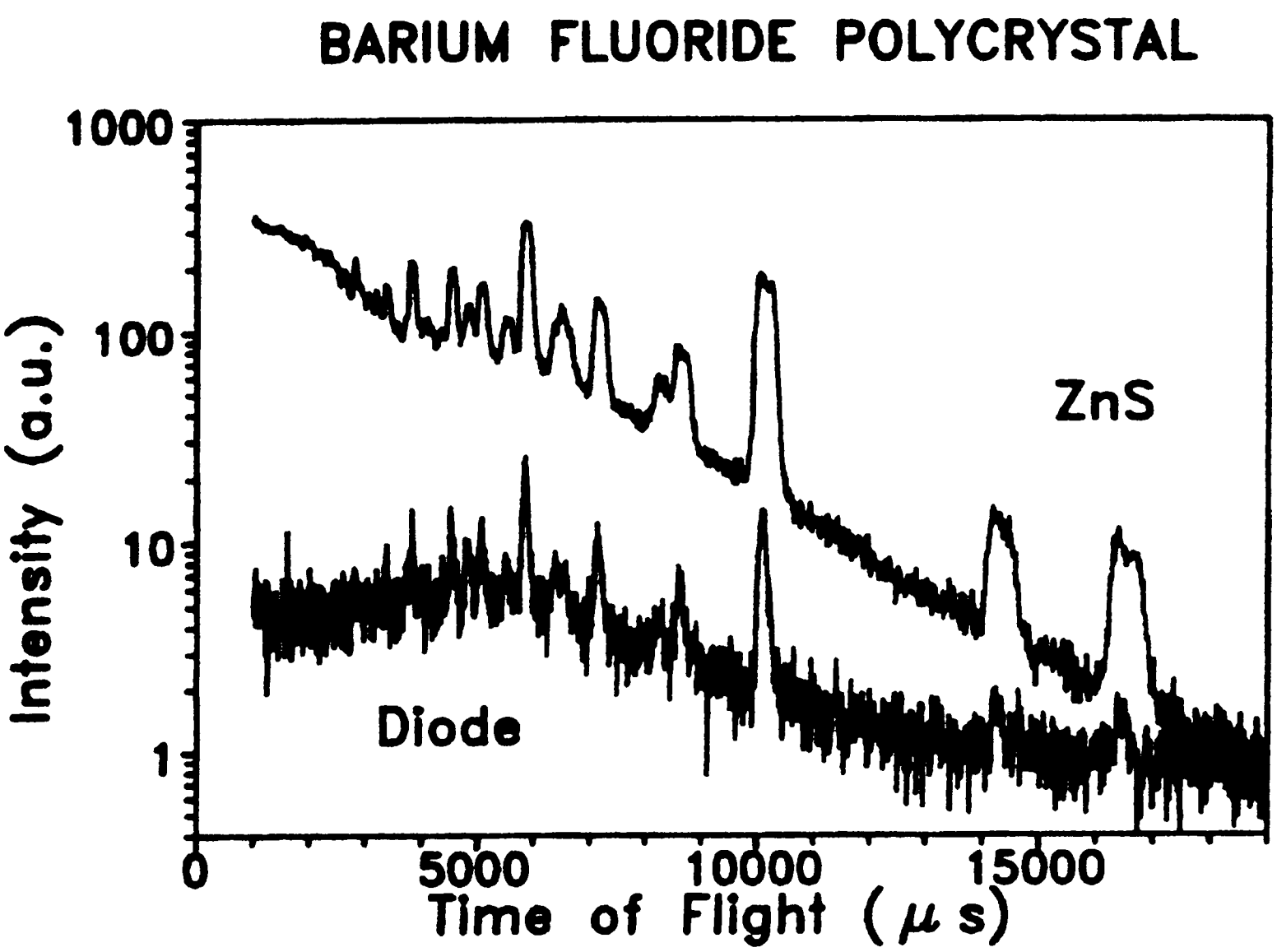

Figure 6b. ToF spectra from the BaF_2 polycrystal.

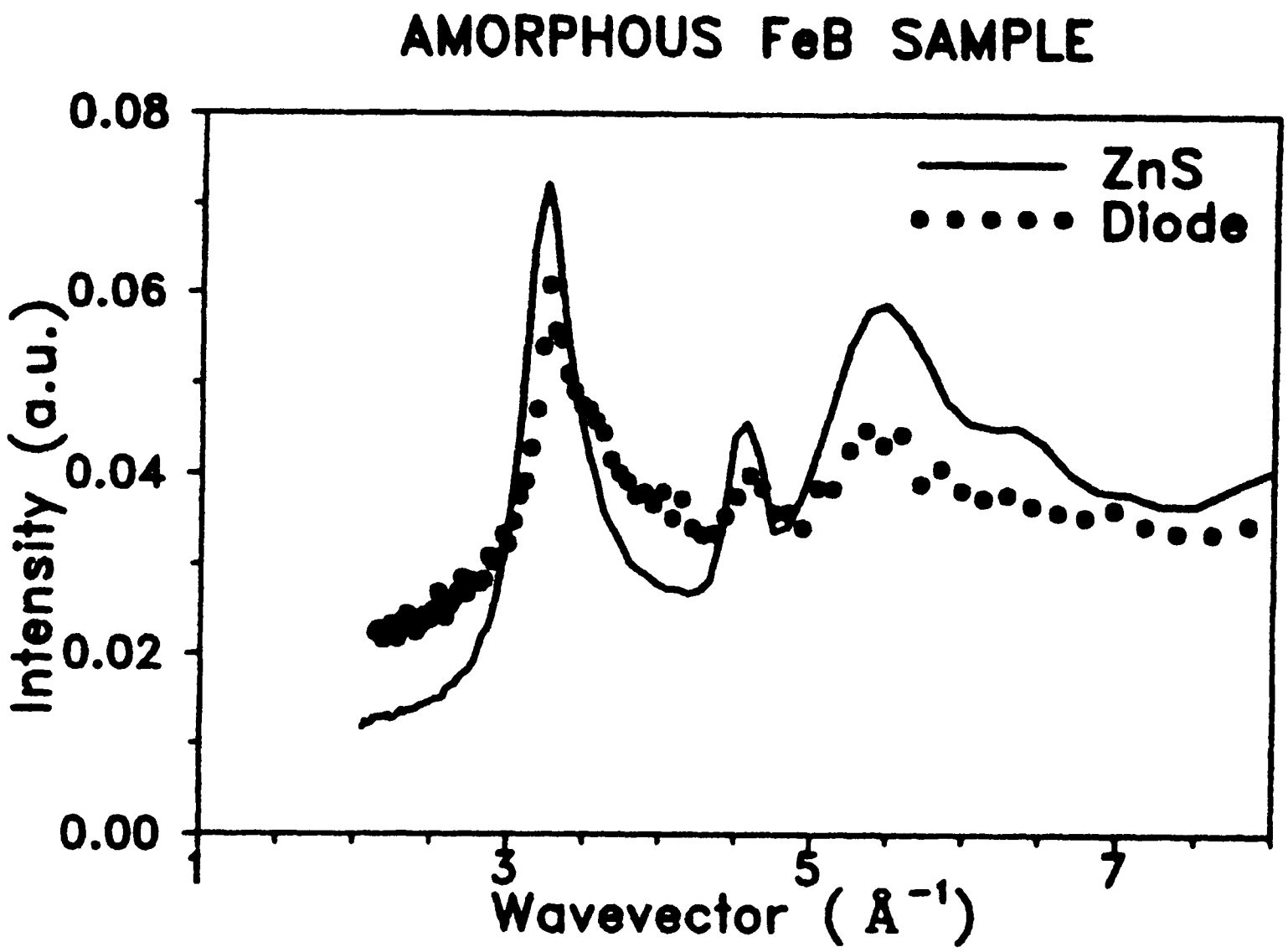

Figure 7. Corrected intensity versus wavevector from the amorphous FeB ribbon (see text) Si detector (dots), ZnS scintillator (full line).

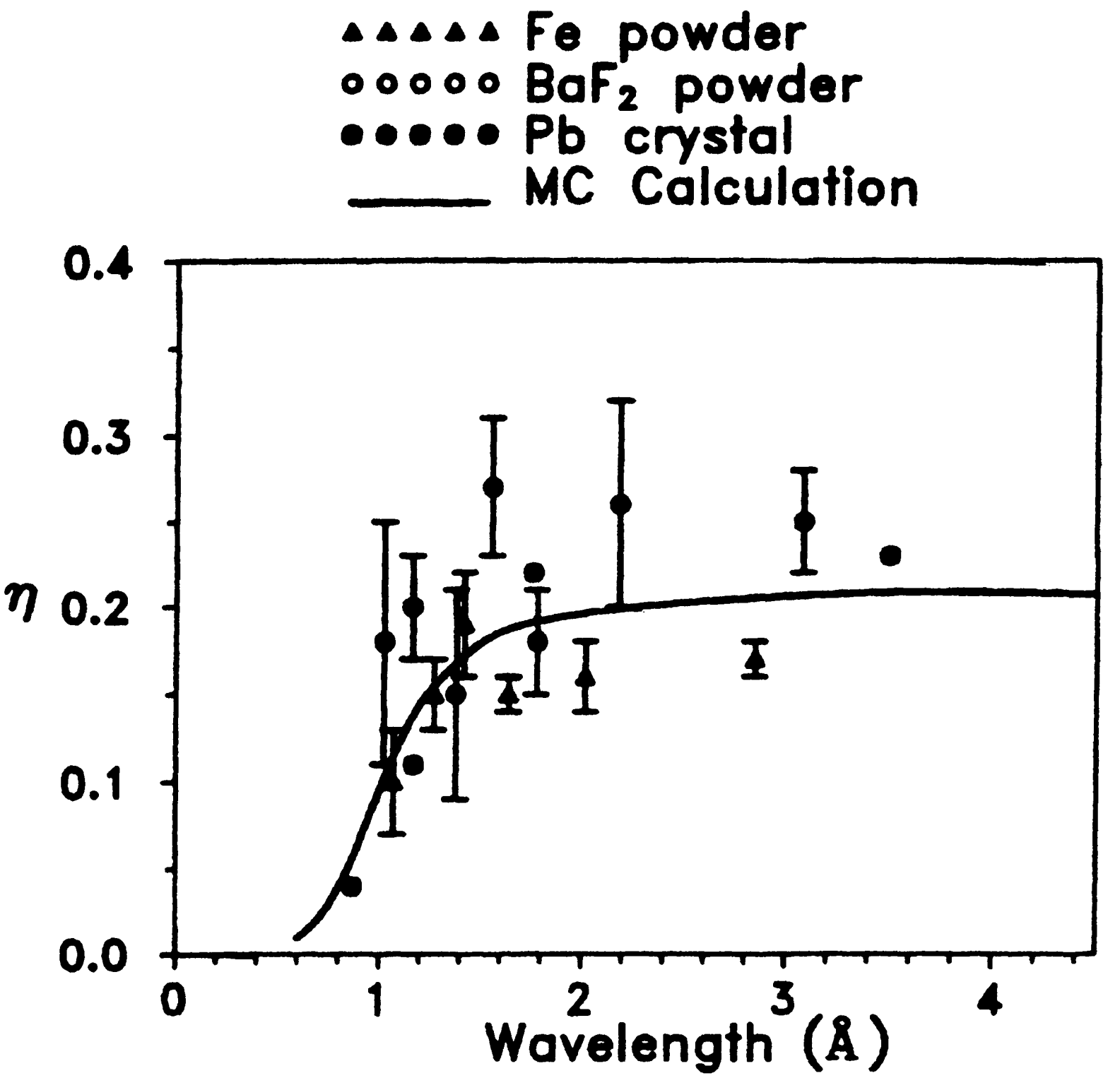

Figure 8a. Experimental neutron detection efficiency calculated using Pb (dots), Fe (triangles) and BaF_2 (circles) data. The full line is the Monte Carlo curve calculated for the present experimental configuration.

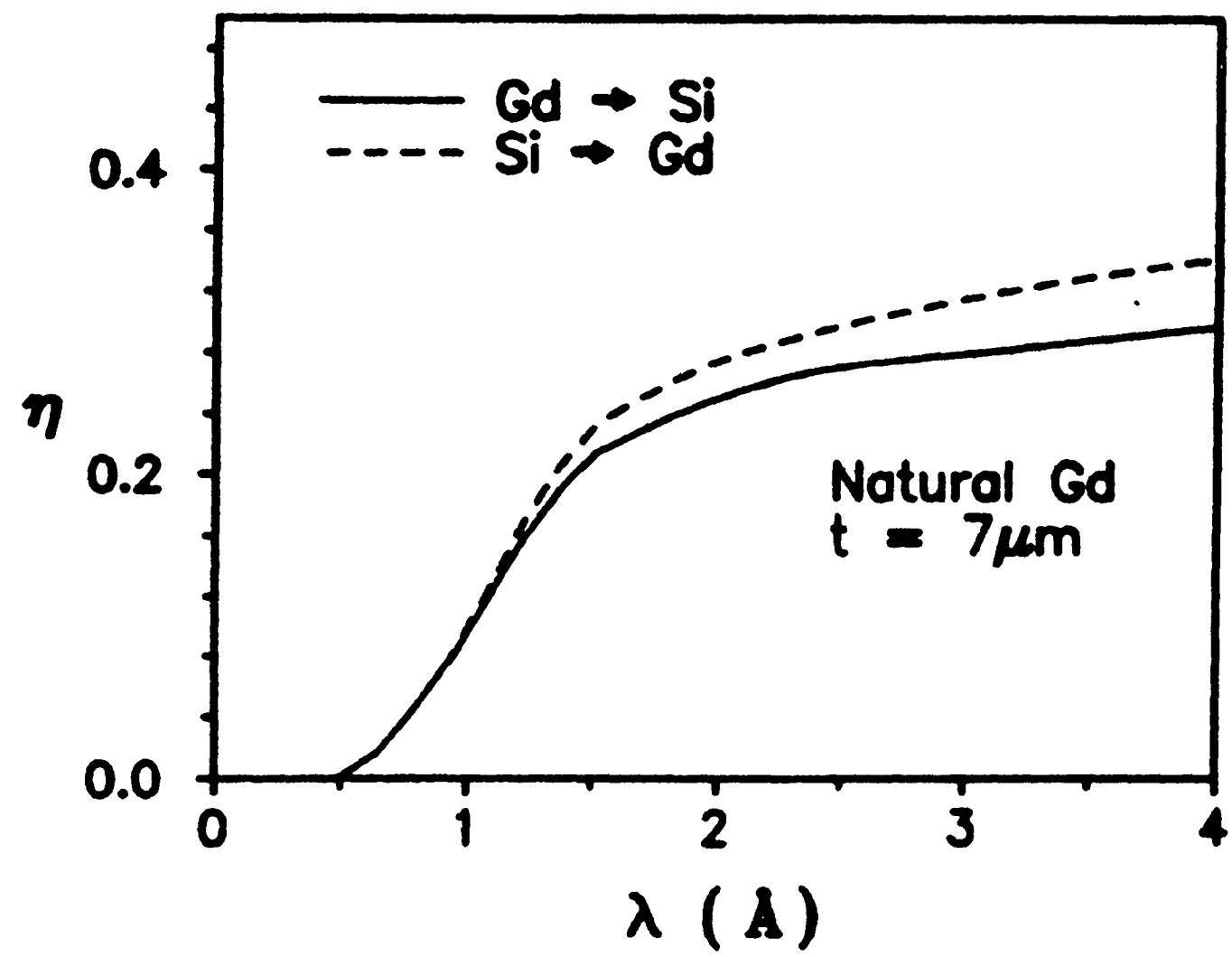

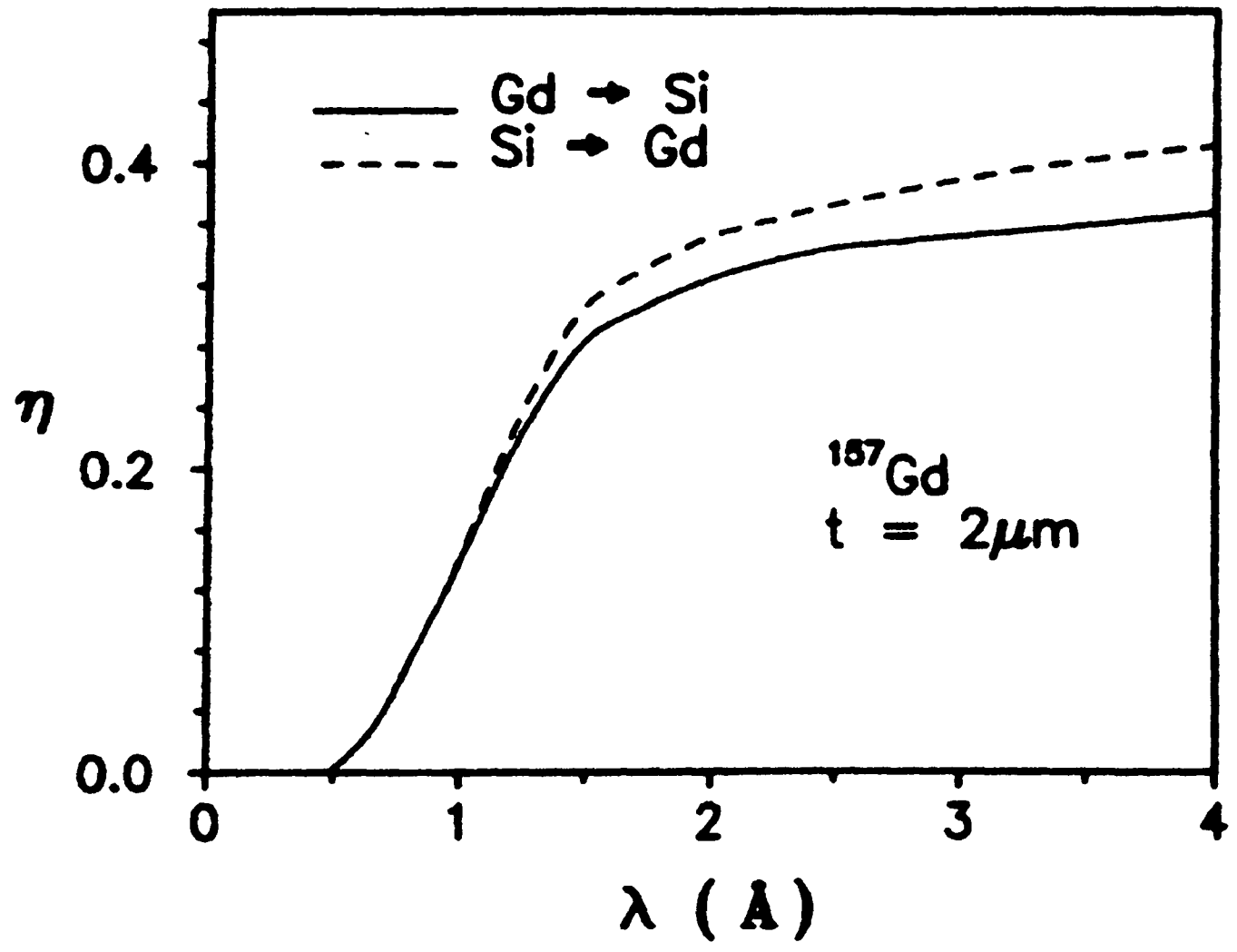

Figure 8b. Monte Carlo simulation of the best performance achievable with the Si detector